

# Alkyne Exchange Reactions of Silylalkyne Complexes of Tantalum: Mechanistic Investigation and Its Application in the Preparation of New Tantalum Complexes Having Functional Alkynes (PhC≡CR (R = COOMe, CONMe<sub>2</sub>))

Toshiyuki Oshiki,\* Atsushi Yamada, Kimio Kawai, Hirotaka Arimitsu, and Kazuhiko Takai\*

Division of Chemistry and Biochemistry, Graduate School of Natural Science and Technology, Okayama University, Tsushima, Okayama 700-8530, Japan

Received July 21, 2006

Silylalkyne complexes of tantalum with the general formula TaCl<sub>3</sub>(R<sup>1</sup>C≡CR<sup>2</sup>)L<sub>2</sub> (**1**, R<sup>1</sup> = R<sup>2</sup> = SiMe<sub>3</sub>, L<sub>2</sub> = DME; **2**, R<sup>1</sup> = SiMe<sub>3</sub>, R<sup>2</sup> = Me, L<sub>2</sub> = DME; **6**, R<sup>1</sup> = R<sup>2</sup> = SiMe<sub>3</sub>, L = py; **7**, R<sup>1</sup> = SiMe<sub>3</sub>, R<sup>2</sup> = Me, L = py) reacted with an internal alkyne to give corresponding alkyne complexes via an alkyne exchange reaction. These silylalkyne complexes were newly prepared and structurally characterized. Kinetic measurements revealed that the rates of the exchange reactions of the DME complexes **1** and **2** were first-order dependent on the concentration of the complex and the reaction proceeded via dissociative pathway. The exchange reaction rates of the bis(pyridine) complexes **6** and **7** were slower. In contrast to the DME complexes, the exchange reaction of **6** proceeded via an associative interchange pathway, and the exchange mechanism for **7** was an associative pathway. During the exchange, two pyridine ligands coordinated strongly to the tantalum center and the intermediate is proposed to be a bis(alkyne) complex. New tantalum complexes having functional alkynes (PhC≡CR (R = COOMe, CONMe<sub>2</sub>)) were prepared from the silylalkyne complexes via the alkyne exchange reaction.

## Introduction

Ligand exchange is a fundamental reaction in the chemistry of transition metal complexes.<sup>1</sup> A complex having an appropriate labile ligand can be used as a suitable starting complex for the preparation of a new complex by a ligand exchange reaction. In addition, the reaction is one of the key steps in the catalytic transformation of organic molecules mediated by transition metal complexes. It has been known that an alkyne ligand coordinated

to a metal center is substitutionally labile even though the ligand usually coordinates strongly as a four-electron-donor ligand.<sup>2</sup> Rosenthal and co-workers have extensively investigated the reactivities of bis(trimethylsilyl)acetylene complexes of titanocene and zirconocene.<sup>3,4</sup> The bis(trimethylsilyl)acetylene ligand can be substituted by various kinds of unsaturated organic molecules to afford the corresponding Cp<sub>2</sub>M derivatives (M = Ti and Zr). Thus, these bis(trimethylsilyl)acetylene complexes serve as an isolable equivalent of a reactive “Cp<sub>2</sub>M” fragment. The lability of the bis(trimethylsilyl)acetylene ligand of titanocene complexes can be applied to the complexes as a precatalyst for hydroamination of alkynes.<sup>5</sup>

We have been investigating the tantalum–alkyne complexes that have no bulky ligand such as cyclopentadienyl and aryloxy groups.<sup>6a,b</sup> These tantalum–alkyne complexes with the general formula TaCl<sub>3</sub>(R<sup>1</sup>C≡CR<sup>2</sup>)L<sub>2</sub> have been prepared and isolated by a one-pot reaction of TaCl<sub>5</sub>, Zn, and alkyne in a mixed solvent of toluene and DME. The substituted group at the alkyne carbon (R<sup>1</sup> and R<sup>2</sup>) is an unreactive hydrocarbon group, trimethylsilyl group, or hydrogen.<sup>6a,b</sup> Previously, we reported that a mixture of an in situ generated low-valent tantalum “TaCl<sub>3</sub>” and alkyne having an ester or amide group (PhC≡CCOOMe or PhC≡CCONMe<sub>2</sub>) reacts with a carbonyl compound to give the corresponding allylic alcohol in high yield

(5) Tillack, A.; Jiao, H.; Garcia Castro, I. Hartung, C. G.; Beller, M. *Chem. Eur. J.* **2004**, *10*, 2409.

(6) (a) Oshiki, T.; Tanaka, K.; Yamada, J.; Ishiyama, T.; Kataoka, Y.; Mashima, K.; Tani, K.; Takai, K. *Organometallics* **2003**, *22*, 464. (b) Oshiki, T.; Nomoto, H.; Tanaka, K.; Takai, K. *Bull. Chem. Soc. Jpn.* **2004**, *77*, 1009. (c) Hierso, J.-C.; Etienne, M. *Eur. J. Inorg. Chem.* **2000**, 839. (d) Guérin, F.; McConville, D. H.; Vittal, J. J.; Yap, C. A. P. *Organometallics* **1998**, *17*, 1290. (e) Strickler, J. R.; Wexler, P. A.; Wigley, D. E. *Organometallics* **1991**, *10*, 118. (f) Curtis, M. D.; Real, J.; Hirpo, W.; Butler, W. M. *Organometallics* **1990**, *9*, 66. (g) Cotton, F. A.; Hall, W. T. *Inorg. Chem.* **1980**, *20*, 2352.

\* Corresponding authors. Fax: +81-86-251-8094. E-mail: oshiki@cc.okayama-u.ac.jp; ktakai@cc.okayama-u.ac.jp.

(1) (a) Crabtree, R. H. *The Organometallic Chemistry of the Transition Metals*, 4th ed.; John Wiley & Sons: New York, 2005. (b) Kettle, S. F. A. *Physical Inorganic Chemistry*; Oxford University Press: New York, 1998.

(2) (a) Brasch, N. E.; Hamilton, I. G.; Krenske, E. H.; Wild, S. B. *Organometallics* **2004**, *23*, 299. (b) Cui, C.; Köpke, S.; Herbst-Irmer, R.; Roesky, H. W.; Noltemeyer, M.; Schmidt, H.-G.; Wrackmeyer, B. *J. Am. Chem. Soc.* **2001**, *123*, 9091. (c) Herrick, R. S.; Leazer, D. M.; Templeton, J. L. *Organometallics* **1983**, *2*, 834. (d) Slater, S.; Muetterties, E. L. *Inorg. Chem.* **1981**, *20*, 1604.

(3) For reviews see: (a) Rosenthal, U.; Burlakov, V. V.; Arndt, P.; Baumann, W.; Spannenberg, A. *Organometallics* **2005**, *24*, 456. (b) Rosenthal, U.; Burlakov, V. V.; Arndt, P.; Baumann, W.; Spannenberg, A.; Shur, V. B. *Eur. J. Inorg. Chem.* **2004**, 4739. (c) Rosenthal, U.; Burlakov, V. V.; Arndt, P.; Baumann, W.; Spannenberg, A. *Organometallics* **2003**, *22*, 884. (d) Rosenthal, U.; Burlakov, V. V. In *Titanium and Zirconium in Organic Synthesis*; Marek, I., Ed.; Wiley-VCH: Weinheim, 2002; p 355. (e) Ohff, A.; Pulst, S.; Lefeber, C.; Peulecke, N.; Arndt, P.; Burlakov, V. V.; Rosenthal, U. *Synlett* **1996**, 111.

(4) (a) Zippel, T.; Arndt, P.; Ohff, A.; Spannenberg, A.; Kempe, R.; Rosenthal, U. *Organometallics* **1998**, *17*, 4429. (b) Ohff, A.; Zippel, T.; Arndt, P.; Spannenberg, A.; Kempe, R.; Rosenthal, U. *Organometallics* **1998**, *17*, 1649. (c) Rosenthal, U.; Ohff, A.; Baumann, W.; Tillack, A.; Görls, H.; Burlakov, V. V.; Shur, V. B. *Z. Anorg. Allg. Chem.* **1995**, 621. (d) Burlakov, V. V.; Polyakov, A. V.; Yanovsky, A. I.; Struchkov, Y. T.; Shur, V. B.; Vol'pin, M. E.; Rosenthal, U.; Görls, H. *J. Organomet. Chem.* **1994**, 476, 197. (e) Rosenthal, U.; Ohff, A.; Michalik, M.; Görls, H.; Burlakov, V. V.; Shur, V. B. *Angew. Chem., Int. Ed. Engl.* **1993**, *32*, 1193.

**Table 1.** Reaction of Internal Alkynes with Tantalum–Alkyne Complexes in C<sub>6</sub>D<sub>6</sub>

entry	complex	alkyne	temp (°C)	time (h)	yield (%) <sup>a</sup>
1	TaCl <sub>3</sub> (Me <sub>3</sub> SiC≡CMe)(dme) ( <b>2</b> )	PhC≡CPh	60	2	>99
2	TaCl <sub>3</sub> (Me <sub>3</sub> SiC≡CSiMe <sub>3</sub> )(dme) ( <b>1</b> )	EtC≡CEt	25	4.5	88
3	TaCl <sub>3</sub> (Me <sub>3</sub> SiC≡CSiMe <sub>3</sub> )(dme) ( <b>1</b> )	PhC≡CPh	25	22	89
4	TaCl <sub>3</sub> (Me <sub>3</sub> SiC≡CSiMe <sub>3</sub> )(dme) ( <b>1</b> )	EtC≡CEt	25	3	93
5	TaCl <sub>3</sub> (EtC≡CEt)(dme) ( <b>4</b> )	Me <sub>3</sub> SiC≡CSiMe <sub>3</sub>	50	10	0
6	TaCl <sub>3</sub> (PhC≡CPh)(dme) ( <b>3</b> )	Me <sub>3</sub> SiC≡CSiMe <sub>3</sub>	50	10	0
7	TaCl <sub>3</sub> (EtC≡CEt)(dme) ( <b>4</b> )	PhC≡CPh	60	12	43
8	TaCl <sub>3</sub> (PhC≡CPh)(dme) ( <b>3</b> )	EtC≡CEt	100 <sup>b</sup>	3	0
9	TaCl <sub>3</sub> (BuC≡CMe)(dme) ( <b>5</b> )	PhC≡CPh	60	12	96
10	TaCl <sub>3</sub> (BuC≡CMe)(dme) ( <b>5</b> )	EtC≡CEt	60	9	18
11	TaCl <sub>3</sub> (BuC≡CMe)(dme) ( <b>5</b> )	EtC≡CEt	25	36	18

<sup>a</sup> Determined by <sup>1</sup>H NMR. <sup>b</sup>Toluene-*d*<sub>8</sub> was used.

with remarkable regioselectivity.<sup>7</sup> The functional alkyne triple bonds certainly coordinate to the tantalum in η<sup>2</sup>-form in situ, because the formation of the allylic alcohols with *E*-form are predominantly formed. An attempt to isolate the TaCl<sub>3</sub>(PhC≡CCOOMe)(dme) complex succeeded only one time by the reaction of TaCl<sub>5</sub> with Zn, PhC≡CCOOMe. However, we have been unable to reproduce it, even though we examined the various reaction and isolation conditions. Thus, our conventional synthetic method for tantalum–alkyne complexes has limitations for isolation of the desired complex having the functionalized alkyne. Development of other synthetic routes to a tantalum–alkyne complex would expand the chemistry of new tantalum–alkyne complexes that have not been isolated to date.

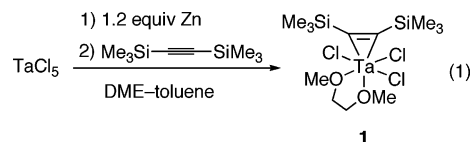
To prepare a new tantalum–alkyne complex, our attention was focused on an alkyne ligand exchange reaction of a silylalkyne complex. As described above, a silylalkyne is a labile ligand for titanocene and zirconocene complexes, and therefore it would be a suitable ligand for an exchange reaction of group 5 tantalum complexes. There are no reports on an alkyne exchange reaction of tantalum–alkyne complexes.

We found that a silylalkyne ligand on the TaCl<sub>3</sub>L<sub>2</sub> fragment was labile, and the ligand was substituted by an internal alkyne such as 3-hexyne or diphenylacetylene. Kinetics studies revealed that the mechanism of the alkyne exchange reaction proceeded via a dissociative mechanism in the case of the DME complex and, in contrast, an associative mechanism for bis(pyridine) complexes. These mechanisms are different from those reported for the alkyne reaction of bis(trimethylsilylacetylene) complexes of titanocene and zirconocene. In addition, new tantalum complexes possessing PhC≡CCOOMe and PhC≡CCONH<sub>2</sub> ligands were prepared using this silylalkyne exchange reaction.

## Results and Discussion

**Preparation of Tantalum–Silylalkyne Complexes.** Preparation of a tantalum–silylalkyne complex was accomplished by a procedure similar to that reported by our group.<sup>6a</sup> Treatment of in situ generated low-valent tantalum “TaCl<sub>3</sub>” with an equimolar amount of bis(trimethylsilyl)acetylene at room temperature for 16 h gave **1** in 28% isolated yield as brown crystals (eq 1). The <sup>13</sup>C{<sup>1</sup>H} NMR spectrum of **1** showed an equivalent signal of two coordinated alkyne carbons at 265.9 ppm. The low-field chemical shift value is comparable to those observed for TaCl<sub>3</sub>(alkyne)L<sub>2</sub> complexes and indicates that the silylalkyne ligand coordinates as an η<sup>2</sup>-four-electron donor ligand.<sup>8</sup> The IR

spectra (ν = 1581 cm<sup>-1</sup>) also support this coordination mode. In spite of the steric bulkiness of the trimethylsilyl group, these spectroscopic data show the silylalkyne ligand rotates rapidly on the tantalum–*trans*-oxygen axis on the NMR time scale. The <sup>1</sup>H NMR spectrum of **1** showed the methyl signal of two trimethylsilyl resonances at δ 0.43 ppm as a singlet peak. Two oxygen atoms of DME coordinate to the tantalum center in a bidentate fashion. To compare our results with previous data, the solution structure of **1** can be described as shown in eq 1. Mono-trimethylsilylalkyne complex TaCl<sub>3</sub>(Me<sub>3</sub>SiC≡CMe)(dme) (**2**) was also prepared using a similar procedure. The solution structure of **2** was essentially the same as that observed for **1**.



**Comparison of the Reactivities of Several Internal Alkyne Complexes in the Alkyne Exchange Reaction.** We examined the alkyne exchange reaction of tantalum–silylalkyne complexes with internal alkynes. Results are summarized in Table 1. The alkyne exchange reaction of TaCl<sub>3</sub>(η<sup>2</sup>-Me<sub>3</sub>SiC≡CMe)(dme) (**2**) with diphenylacetylene proceeded to completion at 60 °C within 2 h, and TaCl<sub>3</sub>(PhC≡CPh)(dme) (**3**) was obtained in quantitative yield. The exchange reaction of bis(trimethylsilyl)acetylene complex **1** proceeded at a lower temperature of 25 °C. After 22 h, complex **3** was obtained in 89% yield. The reactivity of 3-hexyne is greater than that of diphenylacetylene. At 25 °C, the reaction of **1** with 3-hexyne gave TaCl<sub>3</sub>(EtC≡CEt)(dme) (**4**) in 93% yield.

The reactions of **3** or **4** with Me<sub>3</sub>SiC≡CSiMe<sub>3</sub> did not occur in C<sub>6</sub>D<sub>6</sub> at 50 °C for 10 h, and starting complexes remained unchanged after the reactions. Thus, the alkyne exchange reactions of **1** with the internal alkynes are irreversible.

Compared with the Me<sub>3</sub>SiC≡CR (R = SiMe<sub>3</sub>, Me) complexes, the exchange reactions of 3-hexyne complex **3** and diphenylacetylene complex **4** are sluggish. For example, the exchange reaction of **3** with diphenylacetylene proceeded slowly at 60 °C, and **4** was obtained in 43% yield and 57% of **3** remained after 12 h. In contrast, complex **4** did not react with 3-hexyne even at 100 °C. It has been reported that the η<sup>2</sup>-diphenylacetylene ligand of the titanium(II) porphyrin complex cannot be displaced by an aliphatic internal alkyne such as 2-butyne or 3-hexyne, whereas coordinated 2-butyne is capable of exchanging diphenylacetylene from the titanium(II) porphyrin complex.<sup>9</sup> Reactivities of tantalum complexes **3** and **4** are comparable to those of the titanium complexes.

(7) Kataoka, Y.; Miyai, J.; Tezuka, M.; Takai, K.; Utimoto, K. *J. Org. Chem.* **1992**, *57*, 6796.

(8) (a) Templeton, J. L. *Adv. Organomet. Chem.* **1989**, *29*, 1. (b) Theopold, K. H.; Holmes, S. J.; Schrock, R. R. *Angew. Chem. Int. Ed. Engl.* **1983**, *22*, 1010. (c) Tatsumi, K.; Hoffmann, R.; Templeton, J. L. *Inorg. Chem.* **1982**, *21*, 466. (d) Templeton, J. L.; Ward, B. C. *J. Am. Chem. Soc.* **1980**, *102*, 3288.

(9) Wang, X.; Gray, S. D.; Chen, J.; Woo, L. K. *Inorg. Chem.* **1998**, *37*, 5. (b) Woo, K. L.; Hays, J. A.; Young, V. G., Jr.; Day, C. L.; Caron, C.; D'Souza, F.; Kadish, K. M. *Inorg. Chem.* **1993**, *32*, 4186.

Table 2. Crystallographic Data for Tantalum–Alkyne Complexes

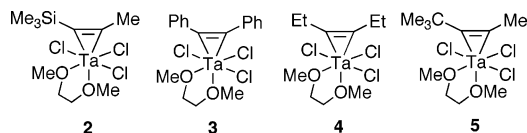
	TaCl <sub>3</sub> (Me <sub>3</sub> SiC≡C-SiMe <sub>3</sub> )(dme) (1)	TaCl <sub>3</sub> (Me <sub>3</sub> Si-C≡CMe)(dme) (2)	TaCl <sub>3</sub> (Me <sub>3</sub> Si-C≡CMe)(py) <sub>2</sub> (7)	TaCl <sub>3</sub> (Pr <sub>3</sub> Si-C≡CMe)(dme) (8)	TaCl <sub>3</sub> (PhC≡C-COOMe)(dme) (9)
formula	C <sub>12</sub> H <sub>28</sub> Cl <sub>3</sub> O <sub>2</sub> Si <sub>2</sub> Ta	C <sub>10</sub> H <sub>22</sub> Cl <sub>3</sub> O <sub>2</sub> SiTa	C <sub>16</sub> H <sub>22</sub> N <sub>2</sub> Cl <sub>3</sub> SiTa	C <sub>16</sub> H <sub>34</sub> Cl <sub>3</sub> O <sub>2</sub> SiTa	C <sub>14</sub> H <sub>18</sub> Cl <sub>3</sub> O <sub>4</sub> Ta
cryst syst	monoclinic	monoclinic	monoclinic	triclinic	monoclinic
space group	<i>P</i> 2 <sub>1</sub> / <i>c</i> (#14)	<i>P</i> 2 <sub>1</sub> (#4)	<i>P</i> 2 <sub>1</sub> / <i>n</i> (#14)	<i>P</i> 1 (#2)	<i>C</i> <i>c</i> (#9)
<i>a</i> , Å	15.981(4)	12.434(2)	9.515(2)	7.6198(4)	8.838(2)
<i>b</i> , Å	7.099(1)	7.4721(6)	13.757(3)	8.0430(3)	19.349(2)
<i>c</i> , Å	18.389(5)	18.098(3)	15.565(2)	20.365(2)	10.576(2)
$\alpha$ , deg				94.342(6)	
$\beta$ , deg	96.084(5)	90.206(2)	95.475(10)	90.295(4)	90.54(2)
$\gamma$ , deg				116.00(1)	
<i>V</i> , Å <sup>3</sup>	2074.5(9)	1681.4(4)	2028.1(7)	1117.5(2)	1808.4(5)
<i>Z</i> value	4	4	4	2	4
<i>D</i> , g/cm <sup>-3</sup>	1.754	1.934	1.827	1.705	1.974
no. of obsd reflns	4548	9426	11 205	7900	2286
no. of variables	182	298	193	203	197
<i>R</i> ; <i>R</i> <sub>w</sub>	0.084, 0.120	0.134, 0.245	0.093, 0.258	0.063, 0.196	0.021, 0.024

Table 3. Selected Bond Distances and Angles for Tantalum–Alkyne Complexes

complex	TaCl <sub>3</sub> (Me <sub>3</sub> SiC≡C-SiMe <sub>3</sub> )(dme) (1)	TaCl <sub>3</sub> (Me <sub>3</sub> SiC≡C-Me)(dme) (2)	TaCl <sub>3</sub> (Me <sub>3</sub> SiC≡C-Me)(py) <sub>2</sub> (7)	TaCl <sub>3</sub> (Pr <sub>3</sub> SiC≡C-Me)(dme) (8)	TaCl <sub>3</sub> (PhC≡C-COOMe)(dme) (9)
C(1)–C(2)	1.326(8)	1.32(2)	1.32(2)	1.32(1)	1.340(9)
Ta–C(1)	2.068(8)	2.11(1)	2.06(1)	2.090(8)	2.055(6)
Ta–C(2)	2.077(5)	2.05(2)	2.08(1)	2.051(9)	2.051(6)
Ta–O(1)	2.183(4)	2.21(1)		2.332(7)	2.189(5)
Ta–O(2)	2.357(4)	2.34(1)		2.240(6)	2.325(4)
Ta–N(1)			2.30(1)		
Ta–N(2)			2.44(1)		
Ta–Cl(1)	2.439(2)	2.428(6)	2.418(4)	2.451(2)	2.388(2)
Ta–Cl(2)	2.377(2)	2.376(9)	2.410(4)	2.382(2)	2.362(2)
Ta–Cl(3)	2.386(2)	2.394(8)	2.381(4)	2.390(2)	2.405(2)
Si(1)–C(1)–C(2)	141.9(5)	140(1)	136(1)	142.6(7)	
Si(2)–C(2)–C(1)	139.8(5)				
C(3)–C(2)–C(1)		139(1)	144(1)	140.2(8)	
C(4)–C(1)–C(2)					138.0(6)
C(3)–C(2)–C(1)					137.4(6)

An alkyne complex having a sterically hindered *tert*-butyl group, TaCl<sub>3</sub>(*t*BuC≡CMe)(dme) (**5**), reacted with diphenylacetylene. Treatment of **5** with diphenylacetylene in C<sub>6</sub>D<sub>6</sub> at 60 °C for 12 h afforded **4** in 96% yield. The reaction of **5** with 3-hexyne was slower, giving **3** in only 18% yield and hexaethylbenzene, which is a cyclotrimerization product of 3-hexyne, in 82% yield based on **5**.

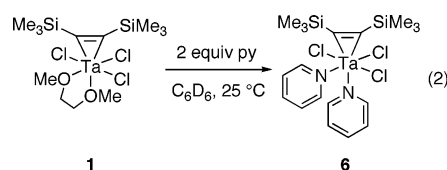
These data indicate that the exchange reactions were accelerated by a silyl group on the coordinated alkyne ligand. In addition, complex **5**, having a sterically hindered *t*Bu group, also assisted the enhancement of the reaction rate.



**Reactivities of Bis(trimethylsilyl)acetylene Complexes with Neutral Donor Ligands.** As reported by Woo et al., a labile alkyne ligand can be substituted by a neutral donor ligand such as pyridine and THF.<sup>9</sup> It has been demonstrated that the DME ligand of tantalum–alkyne complexes is substituted by pyridine, whereas the alkyne ligand is inert in the reaction. For example, when **4** is treated with 2 equiv of pyridine, the DME ligand is exchanged for two pyridines to afford the corresponding bis(pyridine) complex TaCl<sub>3</sub>(EtC≡CEt)(py)<sub>2</sub> in quantitative yield.<sup>6a</sup> The newly prepared silylalkyne complexes exhibit reactivities similar to the reported tantalum–alkyne complexes (vide supra).

A reaction of **1** with 2 equiv of pyridine gave the corresponding bis(pyridine) complex TaCl<sub>3</sub>(Me<sub>3</sub>SiC≡CSiMe<sub>3</sub>)(py)<sub>2</sub> (**6**) in almost quantitative yield without loss of the bistrimethylsilylacetylene ligand (eq 2). Complex **2** also reacted with

pyridine under similar conditions to give the corresponding bis(pyridine) complex TaCl<sub>3</sub>(Me<sub>3</sub>SiC≡CMe)(py)<sub>2</sub> (**7**). The reactions of other monodentate donor ligands were also investigated under various conditions. Treatment of **1** with THF caused the decomposition of the starting complex. In the case of tetrahydrothiophene and trimethylphosphine, the reactions gave a complex mixture of products.



#### X-ray Crystallographic Analysis of Silylalkyne Complexes.

As described above, the silylalkyne ligands of tantalum complexes are labile and the complexes are suitable for alkyne exchange reactions. It is anticipated that this lability is caused by the elongation of the tantalum–silylalkyne bonds. To estimate the strength of the tantalum–silylalkyne bond, X-ray crystallographic analyses of **1**, **2**, **7**, and TaCl<sub>3</sub>(Pr<sub>3</sub>SiC≡CMe)(dme) (**8**) were carried out and their structural parameters compared with those of previously reported tantalum–alkyne complexes. Crystallographic data and structural parameters are listed in Table 2 and Table 3, respectively. Molecular structures are represented in Figures 1–4. For complex **1**, the solid-state structure is comparable with that observed in C<sub>6</sub>D<sub>6</sub> solution. The bis(trimethylsilyl)acetylene ligand coordinates to the tantalum center in  $\eta^2$ -form and two oxygen atoms of the DME ligand occupy *cis* and *trans* positions of the silylalkyne ligand. The bond angles Si(1)–C(1)–C(2) (141.9°) and Si(2)–C(2)–C(1) (139.8(5)°) are bent largely like that of free alkyne. The

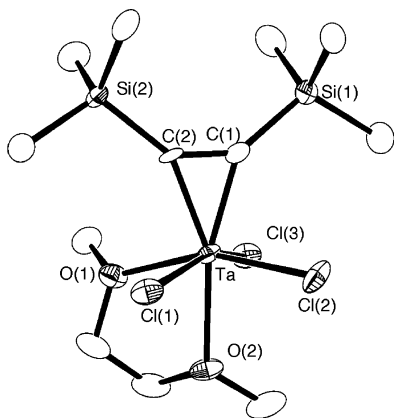


**Figure 1.** Molecular structure of **1**.

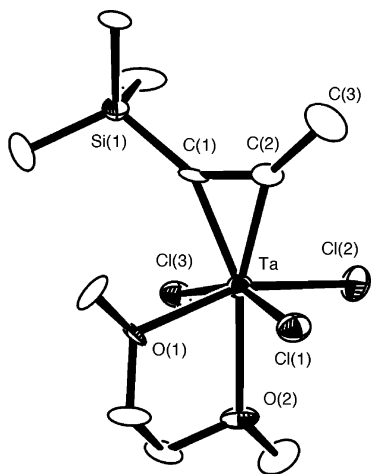


**Figure 2.** Molecular structure of **2**.

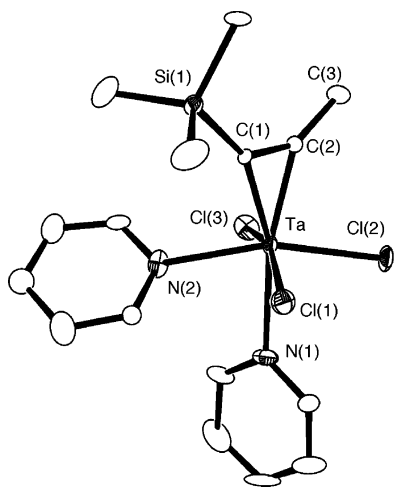


**Figure 3.** Molecular structure of **7**.

C(1)–C(2) distance (1.326(8) Å) is longer than that of a normal C≡C bond (ca. 1.20 Å) and is comparable to that of a normal C–C bond (ca. 1.34 Å). The longer bond distance of Ta–O(2) (2.357(4) Å) compared with Ta–O(1) (2.183(4) Å) can be ascribed to the *trans* influence of the alkyne ligand. Structural parameters of **2**, **7**, and **8** are similar to those of **1**. For **2**, the unit cell contains two independent molecules that do not differ significantly in geometry. Moreover, the bond distances of the tantalum–silylalkyne bond of these complexes are essentially the same as those reported for tantalum–alkyne complexes.<sup>6</sup> Thus, the silylalkyne ligands are actually labile; however, clear

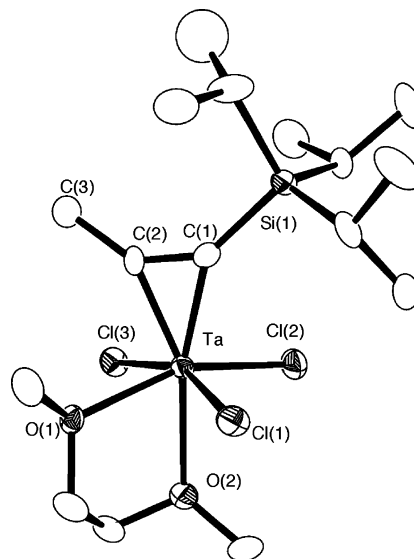


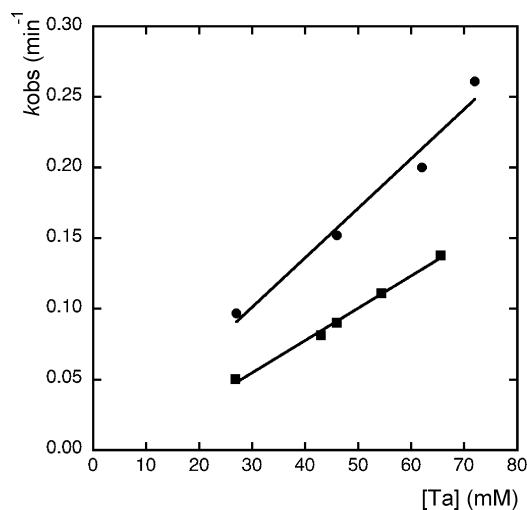
**Figure 4.** Molecular structure of **8**.

evidence for the tantalum–silylalkyne bond weakened by the silyl group could not be found from the solid-state structure.

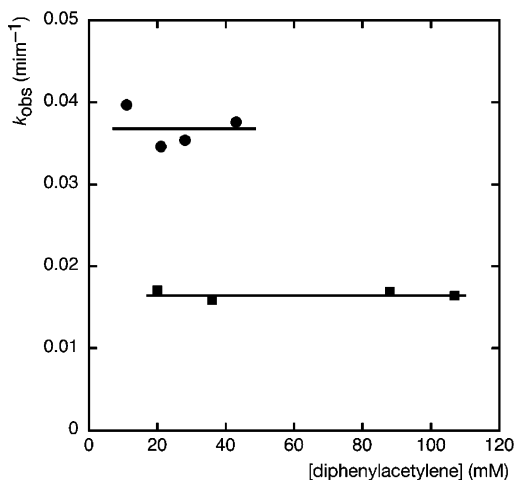
**Kinetics and Thermodynamic Parameters for the Alkyne Exchange Reactions.** During the alkyne exchange reaction, only two tantalum–alkyne complexes and two free alkynes were observed, and no intermediate was detected by <sup>1</sup>H NMR spectroscopy. It has been proposed that an exchange reaction of a Cp<sub>2</sub>Zr–bis(trimethylsilyl)acetylene complex with an alkyne via the associative mechanism occurs.<sup>3</sup> The product, Cp<sub>2</sub>Zr–alkyne complex, would be formed via zirconacyclopentadiene. In contrast, in the case of the Cp<sub>2</sub>Ti–bis(trimethylsilyl)acetylene complex, a dissociative pathway has been strongly supported from the fact that the isolation of the titanocene is generated by the dissociation of the coordinated bis(trimethylsilyl)acetylene from the Cp<sub>2</sub>Ti–bis(trimethylsilyl)acetylene. To elucidate the mechanism for the alkyne exchange reaction of the tantalum complexes, we estimated the kinetics and thermodynamic parameters. The kinetic measurement was carried out in C<sub>6</sub>D<sub>6</sub> under pseudo-first-order conditions, and the reactions were monitored by <sup>1</sup>H NMR spectroscopy.

**Reaction of DME Complexes 1 and 2 with Diphenylacetylene.** The reaction of **1** with diphenylacetylene was determined to be first-order in **1** (Figure 5). The concentration of diphenylacetylene did not affect the rate of the reaction (Figure 6). Activation parameters were obtained by temperature dependence studies. From the Eyring plot (Figure 7),  $\Delta G^\ddagger = +85 \pm 6$  kJ mol<sup>-1</sup> (295.15 K),  $\Delta H^\ddagger = +98 \pm 6$  kJ mol<sup>-1</sup>, and  $\Delta S^\ddagger = +44 \pm 15$  J K<sup>-1</sup>mol<sup>-1</sup>. This positive entropy value indicates that the exchange reaction proceeded via a dissociative mechanism. The kinetics and thermodynamic parameters of the exchange reaction of **2** with diphenylacetylene were similar to those observed for the reaction of **1** with diphenylacetylene (Figures 5 and 6). The reaction proceeded first-order in the concentration of **2**, and the rate was slower than in the case of **1**. Estimated activation parameters for **2** were  $\Delta G^\ddagger = +92 \pm 4$  kJ mol<sup>-1</sup> (295.15 K),  $\Delta H^\ddagger = +100 \pm 4$  kJ mol<sup>-1</sup>, and  $\Delta S^\ddagger = +26 \pm 13$  J K<sup>-1</sup>mol<sup>-1</sup>. Both DME complexes **1** and **2** reacted with diphenylacetylene via a dissociative pathway with positive activation entropy.

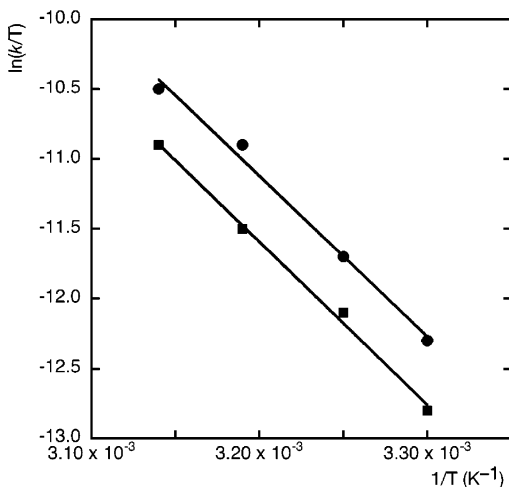
**Reactions of Bis(pyridine) Complexes 6 and 7 with Diphenylacetylene.** The alkyne exchange reaction of bis(pyridine) complexes **6** and **7** is quite different from that of DME complexes. The rate of the reaction can be described as



**Figure 5.** Plot of  $k_{\text{obs}}$  vs concentration of tantalum–silylalkyne complexes for the silylalkyne exchange reaction with diphenylacetylene at 40 °C in  $\text{C}_6\text{D}_6$  (●, complex 1; ■, complex 2).

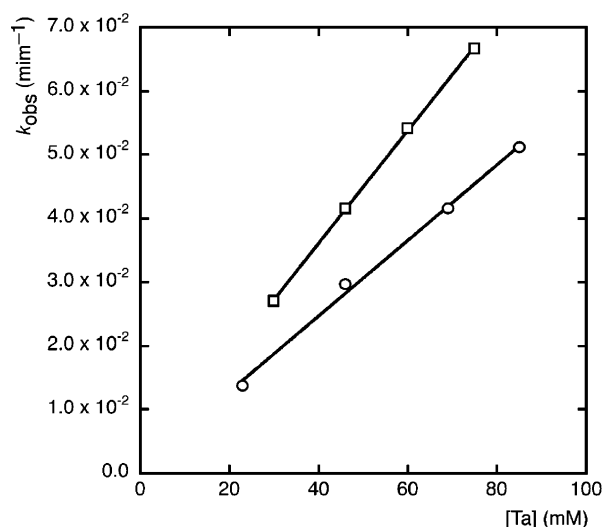


**Figure 6.** Plot of  $k_{\text{obs}}$  vs concentration of diphenylacetylene for the silylalkyne exchange reaction with diphenylacetylene at 40 °C in  $\text{C}_6\text{D}_6$  (●, complex 1; ■, complex 2).

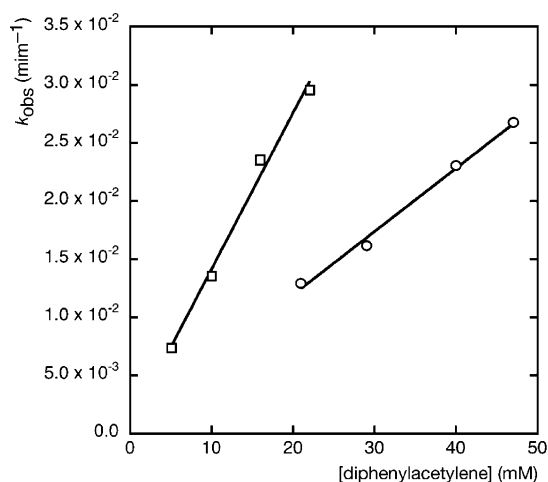


**Figure 7.** Eyring plot of the silylalkyne exchange reactions of **1** and **2** with diphenylacetylene in  $\text{C}_6\text{D}_6$  (●, complex 1; ■, complex 2).

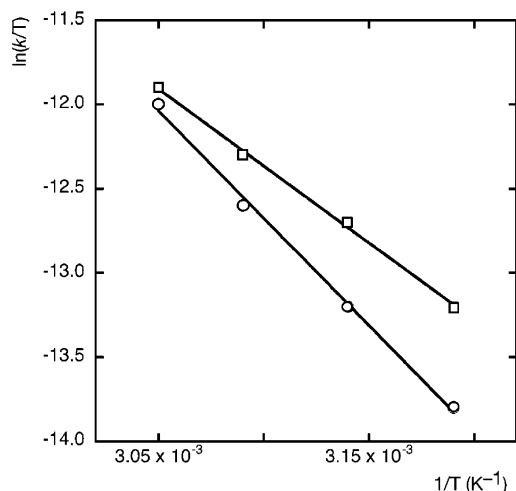
second-order; rate =  $k[\text{Ta complex}][\text{diphenylacetylene}]$  (Figure 8 and Figure 9). As shown in Table 4,  $\Delta G^\ddagger$  and  $\Delta H^\ddagger$  are comparable to the values estimated for **1** and **2**. However,  $\Delta S^\ddagger$  values ( $-1.5 \pm 1.2 \text{ J K}^{-1} \text{ mol}^{-1}$  for **6** and  $-64 \pm 9 \text{ J K}^{-1} \text{ mol}^{-1}$



**Figure 8.** Plot of  $k_{\text{obs}}$  vs concentration of tantalum–silylalkyne complexes for the silylalkyne exchange reaction with diphenylacetylene at 50 °C in  $\text{C}_6\text{D}_6$  (□, complex 6; ○, complex 7).



**Figure 9.** Plot of  $k_{\text{obs}}$  vs concentration of diphenylacetylene for the silylalkyne exchange reaction with diphenylacetylene at 60 °C in  $\text{C}_6\text{D}_6$  (□, complex 6; ○, complex 7).

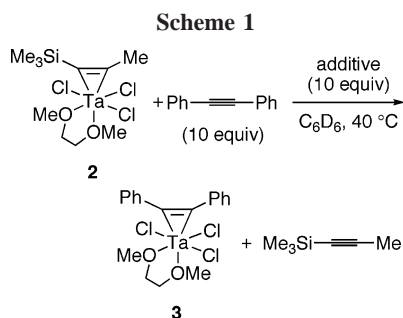


**Figure 10.** Eyring plot of the silylalkyne exchange reactions of **6** and **7** with diphenylacetylene in  $\text{C}_6\text{D}_6$  (□, complex 6; ○, complex 7).

for **7**) suggest that the exchange mechanism is different from that in the case of **1** and **2**. For **7**, the negative  $\Delta S^\ddagger$  indicates that the exchange proceeded via an associative mechanism. The

**Table 4.** Activation Parameters for the Ligand Exchange Reactions of Tantalum Complexes with Diphenylacetylene

complex	$\Delta G^\ddagger$ (kJ mol <sup>-1</sup> ) <sup>a</sup>	$\Delta H^\ddagger$ (kJ mol <sup>-1</sup> )	$\Delta S^\ddagger$ (J K <sup>-1</sup> mol <sup>-1</sup> )
TaCl <sub>3</sub> (Me <sub>3</sub> SiC≡CSiMe <sub>3</sub> )(dme) ( <b>1</b> )	+85 ± 6	+98 ± 6	+44 ± 15
TaCl <sub>3</sub> (Me <sub>3</sub> SiC≡CMe)(dme) ( <b>2</b> )	+92 ± 4	+100 ± 4	+26 ± 13
TaCl <sub>3</sub> (Me <sub>3</sub> SiC≡CSiMe <sub>3</sub> )(py) <sub>2</sub> ( <b>6</b> )	+98 ± 0	+97 ± 0	-1.5 ± 1.2
TaCl <sub>3</sub> (Me <sub>3</sub> SiC≡CMe)(py) <sub>2</sub> ( <b>7</b> )	+95 ± 3	+76 ± 3	-4 ± 9

<sup>a</sup> 298.15 K.

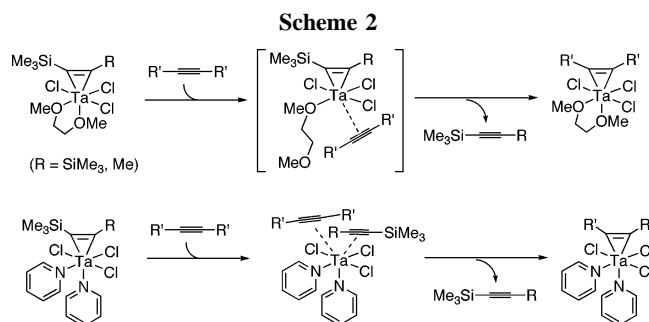
additive	$k_{\text{obs}}$ ( $\times 10^{-2} \text{ min}^{-1}$ )
none	9.04 ± 0.39
Me <sub>3</sub> Si-C≡C-Me	4.56 ± 0.19
DME	0 (no reaction)
	2.39 ± 0.05

interpretation of  $\Delta S^\ddagger$  for **6**, which is essentially zero, which will be discussed later.

**Effects of Additives in the Alkyne Exchange Reactions of 2.** To reveal the further mechanistic details of the exchange reactions, the effect of an additive in the reaction was investigated. As described above, kinetic measurements of the reaction of **2** suggested a dissociative mechanism. If the exchange reaction proceeded via a ligand dissociation from the tantalum center of **2**, the rate should be strongly affected in the presence of a donor molecule, such as trimethylsilylpropyne or DME.

The reaction of **2** with 10 equiv of diphenylacetylene was carried out in the presence of an additive (additive/**2** = 10) in C<sub>6</sub>D<sub>6</sub> at 40 °C (Scheme 1). The rate became slower when trimethylsilylpropyne was added. The exchange reaction was inhibited completely by addition of DME. To exclude the possibility of inhibition of the exchange reaction by solvent effects of polar DME, cyclopentyl methyl ether, which is a polar solvent like DME, was added to the reaction. Before this experiment, we confirmed that no reaction occurred when **2** was treated with excess cyclopentyl methyl ether. When 10 equiv of cyclopentyl methyl ether was added to the reaction, the exchange proceeded and the rate decreased to  $(2.39 \pm 0.05) \times 10^{-2} \text{ min}^{-1}$ . This result indicates that the alkyne exchange reaction proceeds in both nonpolar (C<sub>6</sub>D<sub>6</sub>) and polar solvents. Cyclopentyl methyl ether is known to be a weakly coordinating solvent; however, its oxygen atom would coordinate weakly to the tantalum center in the exchange reaction to fill a vacant coordination site. The dissociation of the coordinated DME would be a crucial step for the exchange reaction.

**Reaction of TaCl<sub>3</sub>(Pr<sub>3</sub>SiC≡CMe)(dme) (**8**) with Diphenylacetylene.** To estimate the influence of the steric bulkiness of the alkyne substituent, the reaction of **8** with diphenylacetylene was investigated. Complex **8** was prepared as reddish-brown crystals in 17% isolated yield. Kinetic measurements were carried out under 46 mM C<sub>6</sub>D<sub>6</sub> at 40 °C. The rate ( $k_{\text{obs}} = (1.76 \pm 0.05) \times 10^{-1} \text{ min}^{-1}$ ) was faster than that of **2** under the same reaction conditions ( $k_{\text{obs}} = (9.03 \pm 0.39) \times 10^{-2}$



min<sup>-1</sup>). Sterical bulkiness on the silyl group enhances the rate of the exchange reaction, and the elimination of the silylalkyne is a rate-determining step for the alkyne exchange reaction.

**Mechanistic Consideration of the Alkyne Exchange Reactions.** The rate of the alkyne exchange reactions of the DME complexes **1** and **2** is first-order in the complex and zero-order in the alkyne. The reaction pathway is considered to proceed via a dissociative mechanism. The positive  $\Delta S^\ddagger$  value and the rate decrease in the presence of an excess amount of the silylalkyne (Scheme 1), which also supports the mechanism. From the X-ray crystallographic analysis, the structural parameters of the tantalum–silylalkyne fragments are comparable with those observed for nonlabile tantalum–alkyne complexes. Thus, dissociation of the  $\eta^2$ -coordinated silylalkyne occurring in the first step can be excluded.

Scheme 2 illustrates the proposed mechanism of the alkyne exchange reaction. We suppose the dissociation of the oxygen atom of the coordinated DME ligand occurs in the first step of the reaction. The Ta–O bond *trans* to the silylalkyne would cleave because of the bond elongation due to the *trans* influence of the silylalkyne ligand.<sup>6a</sup> A free alkyne ligand can bind rapidly at the generated vacant site to give a corresponding bis(alkyne) intermediate. The hemilability of the DME ligand is supported by the fact that the coordinated DME ligand slowly dissociates from **1** and **2**, and then the complexes gradually decompose in C<sub>6</sub>D<sub>6</sub> solution at room temperature. After the solution was allowed to stand at room temperature overnight, about 5% of the complex decomposed and a colorless precipitate was deposited, which was probably decomposed inorganic salts. The positive  $\Delta S^\ddagger$  of **1** is larger than that of **2**, suggesting that the rate-determining step is the dissociation of the coordinated silylalkyne ligand. The difference in the  $\Delta S^\ddagger$  values indicates that the bis(trimethylsilyl)acetylene ligand of **1** dissociates more easily than the 1-trimethylsilyl-1-propyne of **2** due to its steric bulkiness. The faster exchange reaction rate of **8**, which has a bulky 1-(triisopropylsilyl)-1-propyne compared with **2**, provides additional support for the rate-determining step.

In contrast, in the DME complexes, the exchange reaction pathway of bis(pyridine) complexes is quite different. The associative mechanism can be proposed because second-order kinetics were observed. The rates were found to depend on the concentration of the complex and that of the alkyne.

The negative  $\Delta S^\ddagger$  value for **7** ( $-64 \pm 9 \text{ J K}^{-1} \text{ mol}^{-1}$ ) also supports the associative mechanism.<sup>1</sup> For **6**, the kinetic data clearly indicate that the alkyne exchange reaction proceeds via

an associative pathway; however, the  $\Delta S^\ddagger$  value is essentially zero ( $-1.5 \pm 1.2 \text{ J K}^{-1} \text{ mol}^{-1}$ ). Compared with the exchange reaction of **7**, whose  $\Delta S^\ddagger$  is negative, it would be difficult for diphenylacetylene to approach the tantalum center, because the coordinated bis(trimethylsilyl)acetylene ligand of **6** is bulkier than the trimethylsilylpropyne ligand of **7**. We conclude that the alkyne exchange reaction of **6** is an associative interchange pathway.<sup>1b</sup> For both exchange reactions of **6** and **7**, we observed no free pyridine during the exchange reaction. Two pyridine ligands coordinated strongly to the tantalum center during the exchange reaction. In contrast to the DME complexes, both **6** and **7** are stable in a  $\text{C}_6\text{D}_6$  solution at room temperature under argon and the alkyne exchange reaction of **6** and **7** proceeds via an essentially associative pathway without dissociation of the coordinated pyridine. The reaction proceeds via a seven-coordinate<sup>11</sup> bis(alkyne) intermediate, as depicted in Scheme 2. The intermediate possesses two alkynes as a 2e donor ligand, and thus, it is a formally 16e complex.

It is possible that the alkyne ligand inserts into the tantalum–silylalkyne bond to give a tantalacyclopentadiene complex.<sup>12</sup> In both our DME and bis(pyridine) complexes, no tantalacyclopentadiene was observed in the NMR spectra under various conditions. The reaction proceeds via a bis(alkyne) complex as an intermediate without the formation of the tantalacyclopentadiene. Formation of the bis(alkyne) intermediate was supported by the fact that bis(alkyne) complexes of niobium<sup>13</sup> and tantalum<sup>13c</sup> were reported.

**Alkyne Exchange Reaction of Other Unsaturated Organic Compounds.** The alkyne exchange reaction of the tantalum–silylalkyne complex shows that the complex of type  $\text{TaCl}_3(\text{R}_3\text{SiC}\equiv\text{CR})(\text{dme})$  can be considered as a “ $\text{TaCl}_3(\text{dme})$ ” equivalent. We attempted to apply the exchange reaction to prepare the new tantalum complexes. In sharp contrast to Rosenthal’s group 4 complexes,<sup>3,4</sup> the ligand exchange reactions of **1** with olefinic compounds failed. No reaction occurred when **1** was treated by ethylene (1 atm) at room temperature for 5 days. Dienes (1,4-diphenyl-1,3-butadiene (100 °C, 7 h), isoprene (50 °C, 16 h), norbornadiene (50 °C, 18 h), and fullerene (100 °C, 7 h) were also inactive even at higher temperatures. It is interesting to note that aldimine,  $\text{PhCH}=\text{NCH}_2\text{Ph}$ , did not react with **1** at 50 °C for 16 h, even though the  $\eta^2$ -aldimine complex  $\text{TaCl}_3(\text{PhCH}=\text{NCH}_2\text{Ph})(\text{dme})$  was already isolated by the reaction with  $\text{TaCl}_5$ .<sup>14</sup> Treatment of **1** with diazadiene  $\text{MeOC}_6\text{H}_4\text{N}=\text{CH}-\text{CH}=\text{NC}_6\text{H}_4\text{OMe}$  gave no exchanged product. The silylalkyne ligands of our tantalum complexes were exchanged by an internal alkyne chemoselectively. Comparing the reactivities of  $\text{Cp}_2$ -bis(trimethylsilyl)acetylene ( $\text{M} = \text{Ti}, \text{Zr}$ ), the silylalkyne exchange of the tantalum complex needs a higher temperature. The silylalkyne ligand coordinates more strongly to the  $\text{TaCl}_3\text{L}_2$  fragment than the group 4 metallocene fragment, probably because the tantalum center is more electron deficient than a group 4 metal center having two electron-rich cyclopentadienyl ligands.

(10) (a) Horáček, M.; Kupfer, V.; Thewalt, U.; Štěpnička, P.; Polášek, M.; Mach, K. *Organometallics* **1999**, *18*, 3572. (b) Hitchcock, P. B.; Kerton, F. M.; Lawless, G. A. *J. Am. Chem. Soc.* **1998**, *120*, 10264.

(11) Seven-coordinate tantalum complexes were reported. (a) Chisholm, M. H.; Cotton, F. A.; Extine, M. W. *Inorg. Chem.* **1978**, *7*, 2000. (b) Drew, G. B. M.; Wilkins, J. D. *J. Chem. Soc., Dalton Trans.* **1974**, *18*, 1973.

(12) Strickler, J. R.; Wexler, P. A.; Wigley, D. E. *Organometallics* **1988**, *7*, 2067.

(13) (a) Lorente, P.; Etienne, M.; Donnadiou, B. *Anal. Chim. Acta* **1996**, *92*, 88. (b) Felten, C.; Rehder, D.; Pampaloni, G.; Calderazzo, F. *Inorg. Chim. Acta* **1992**, *202*, 121. (c) Alt, H.; Engelhardt, H. E. Z. *Naturforsch. Teil B* **1987**, *42*, 711.

(14) Takai, K.; Ishiyama, T.; Yasue, H.; Nobunaka, T.; Itoh, M.; Oshiki, T.; Mashima, K.; Tani, K. *Organometallics* **1998**, *17*, 5128.

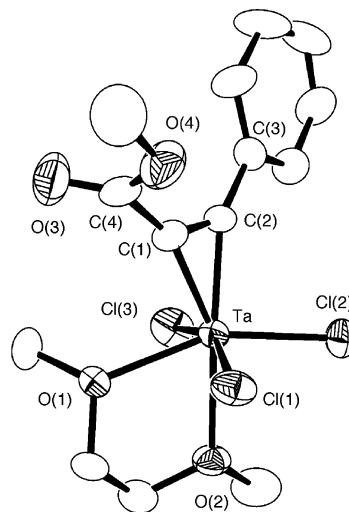
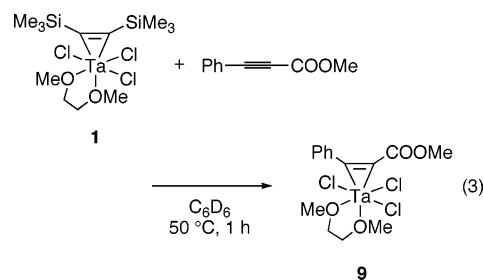
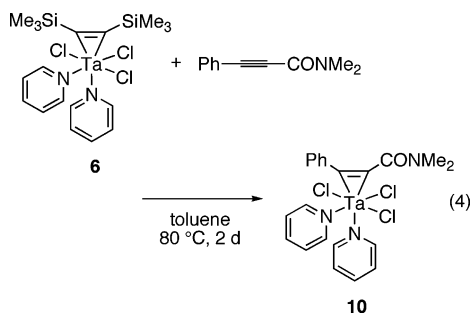


Figure 11. Molecular structure of **9**.

**Preparation of Tantalum Complexes Having Functional Alkynes ( $\text{PhC}\equiv\text{CR}$  ( $\text{R} = \text{COOMe}, \text{CONMe}_2$ )).** As described in the Introduction, we could not prepare a tantalum complex having a  $\text{PhC}\equiv\text{CCOOMe}$  ligand by the reaction of  $\text{TaCl}_5$ , Zn, and  $\text{PhC}\equiv\text{CCOOMe}$ . The reaction of **1** with  $\text{PhC}\equiv\text{CCOOMe}$  successfully proceeded at 50 °C for 1 h to give  $\text{TaCl}_3(\text{PhC}\equiv\text{CCOOMe})(\text{dme})$  (**9**) in 82% isolated yield (eq 3). By monitoring the reaction using  $^1\text{H}$  NMR, it was found that the reaction proceeded quantitatively. Reaction of **2** with  $\text{PhC}\equiv\text{CCOOMe}$  also afforded **1**; however, the reaction was sluggish and uncharacterized byproducts were observed in an NMR tube reaction. The molecular structure of **9** was revealed by X-ray crystallographic analysis. Complex **9** is a discrete molecule and no interaction was observed between the ester group and the tantalum center (Figure 11). The bond distances and angles around the tantalum center are comparable to those found in other tantalum–alkyne complexes.<sup>6</sup>



Preparation of  $\text{PhC}\equiv\text{CCONMe}_2$  complex **10** was accomplished by the reaction of bis(pyridine) complex **6** with  $\text{PhC}\equiv\text{CCONMe}_2$ . A mixture of **6** and  $\text{PhC}\equiv\text{CCONMe}_2$  stirred at 80 °C for 2 days gave **10** in 45% isolated yield (eq 4). When the reaction was monitored by  $^1\text{H}$  NMR, 87% yield of **10** was detected under the same conditions in  $\text{C}_6\text{D}_6$ . Complex **10** was not obtained by the reactions of DME-coordinated silylalkyne complexes **2**. During the reaction, the starting complex **2** was observed to decompose and a free DME ligand was detected. Considering the mechanistic insight of the exchange reaction, the labile DME ligand would be replaced by a polar amido group of  $\text{PhC}\equiv\text{CCONMe}_2$ , and then the exchange reaction would not proceed. In the case of **6**, two strongly coordinated pyridine ligands could not be replaced by the polar amide ligand, allowing the desired **10** to be obtained by the exchange reaction.



## Conclusion

We synthesized and characterized several silylalkyne complexes of tantalum, which reacted with internal alkynes to give the corresponding alkyne complexes via alkyne exchange reactions under mild conditions. Kinetics and thermodynamic parameters revealed the mechanistic insights of the reactions. The difference in neutral ligands of the tantalum–silylalkyne complexes gave different reaction pathways. In the case of the tantalum–silylalkyne DME complexes, dissociation of the labile DME occurred and the exchange reaction proceeded with a positive entropy of activation. In contrast, the pyridine ligands of the tantalum–silylalkyne bis(pyridine) complexes coordinated to the tantalum strongly, and the exchange reaction proceeded via a seven-coordinate bis(alkyne) intermediate with negative entropy of activation. We prepared new tantalum complexes having functional alkynes using the exchange reactions with the silylalkyne complexes.

## Experimental Section

**General Methods and Chemicals.** All manipulations involving air- and moisture-sensitive compounds were carried out using standard Schlenk techniques under an argon atmosphere. Anhydrous hexane, THF, and toluene were purchased from Wako Pure Chemical Industries, Ltd. and stored on 4 Å molecular sieves under argon. Anhydrous 1,2-Dimethoxyethane was purchased from Kanto Chemicals and stored on 4 Å molecular sieves under argon. TaCl<sub>5</sub> was purchased from Nacalai Tesque and used as received. Bis(trimethylsilyl)acetylene and 1-trimethylsilyl-1-propyne were purchased from Aldrich and used after distillation. 4,4-Dimethyl-2-pentyne was purchased from Lancaster and used after distillation. <sup>1</sup>H and <sup>13</sup>C{<sup>1</sup>H} NMR spectra were recorded at 399.65 and 100.40 MHz, respectively, on a JEOL JNM-LA400 spectrometer. The <sup>1</sup>H and <sup>13</sup>C{<sup>1</sup>H} NMR chemical shifts were relative to tetramethylsilane; the resonance of the residual protons of C<sub>6</sub>D<sub>6</sub> was used as an internal standard (δ 7.20 ppm benzene for <sup>1</sup>H and 128.0 ppm benzene for <sup>13</sup>C{<sup>1</sup>H}). IR spectra were recorded by using a Nicolet PROTÉGÉ 460. Melting points were measured in a sealed tube on a Yanaco MP-S3 apparatus and were uncorrected. Elemental analyses were performed at RIKEN.

**TaCl<sub>5</sub>(Me<sub>3</sub>SiC≡CSiMe<sub>3</sub>)(dme) (1).** Toluene (5 mL) was added to TaCl<sub>5</sub> (517 mg, 1.44 mmol) in an 80 mL Schlenk tube, and then DME (10 mL) was slowly added to the resulting yellow suspension. Zn powder (113 mg, 1.73 mmol) was added to the mixture in one portion at room temperature. After stirring the mixture at room temperature for 30 min, bis(trimethylsilyl)acetylene (0.32 mL, 1.44 mmol) was added to the mixture, and the suspension was stirred at

room temperature for 16 h. The resulting insoluble inorganic salts were removed by centrifugation, and the supernatant was transferred to a Schlenk tube. All volatiles were removed in vacuo, and the resulting brown solid was dissolved in toluene (10 mL). After centrifugation, petroleum ether (5 mL) was slowly added to the brown supernatant and placed in a –20 °C freezer overnight, during which brown crystals were deposited. Removal of the supernatant by a syringe and washing the crystals with petroleum ether afforded 224 mg (0.409 mmol) in 28% yield.

Mp: 125–130 °C (dec). IR (nujol/CsI): 1581, 1246, 1024, 932, 839, 752, 377, 302 cm<sup>-1</sup>. <sup>1</sup>H NMR (toluene-*d*<sub>8</sub>): δ 0.43 (s, 18H), 3.08–3.14 (m, 4H), 3.11 (s, 3H), 3.53 (s, 3H). <sup>13</sup>C{<sup>1</sup>H} NMR (toluene-*d*<sub>8</sub>): δ 0.68, 62.24, 67.85, 70.36, 75.67, 265.93. Anal. Calcd for C<sub>12</sub>H<sub>28</sub>Cl<sub>3</sub>O<sub>2</sub>Si<sub>2</sub>Ta: C, 26.31; H, 5.15. Found: C, 26.02; H, 4.87.

**TaCl<sub>5</sub>(Me<sub>3</sub>SiC≡CMe)(dme) (2).** Toluene (30 mL) was added to TaCl<sub>5</sub> (1.70 g, 4.74 mmol) in an 80 mL Schlenk tube, and then DME (12 mL) was slowly added to the resulting yellow suspension. Zn powder (372 mg, 5.69 mmol) was added to the mixture in one portion at room temperature. After stirring the mixture at room temperature for 30 min, 1-trimethylsilyl-1-propyne (710 μL, 4.74 mmol) was added and the suspension was stirred at room temperature for 1 day. The resulting insoluble inorganic salts were removed by centrifugation, and the reddish-brown supernatant was transferred to a Schlenk tube. All volatiles were removed in vacuo, and the resulting brown solid was dissolved in toluene (20 mL). After centrifugation, hexane (20 mL) was slowly added to the supernatant and placed in a –20 °C freezer for 2 days, during which reddish-brown crystals were deposited. Removal of the supernatant by a syringe and washing the crystals with hexane afforded 1.34 g (2.80 mmol) in 59% yield.

Mp: 88–95 °C (dec). IR (nujol/CsI): 1640, 311 cm<sup>-1</sup>. <sup>1</sup>H NMR (C<sub>6</sub>D<sub>6</sub>): δ 0.49 (s, 9H), 3.11–3.12 (m, 4H), 3.14 (s, 3H), 3.47 (s, 3H), 3.67 (s, 3H). <sup>13</sup>C{<sup>1</sup>H} NMR (C<sub>6</sub>D<sub>6</sub>): δ 0.3, 28.6, 62.5, 68.1, 70.5, 75.7, 252.8, 262.6. Anal. Calcd for C<sub>10</sub>H<sub>22</sub>Cl<sub>3</sub>O<sub>2</sub>SiTa: C, 24.53; H, 4.53. Found: C, 24.42; H, 4.53.

**TaCl<sub>5</sub>(BuC≡CMe)(dme) (5).** Toluene (10 mL) was added to TaCl<sub>5</sub> (712 mg, 1.99 mmol) in an 80 mL Schlenk tube, and then DME (10 mL) was slowly added to the resulting yellow suspension. Zn powder (131 mg, 2.34 mmol) was added to the mixture in one portion at room temperature. After stirring the mixture at room temperature for 30 min, 4,4-dimethyl-2-pentyne (257 μL, 1.99 mmol) was added and the suspension was stirred at room temperature overnight. The resulting insoluble inorganic salts were removed by centrifugation, and the supernatant was transferred to a Schlenk tube. All volatiles were removed in vacuo, and the resulting brown solid was dissolved in toluene (5 mL). After centrifugation, hexane (10 mL) was slowly added to the supernatant and placed in a –20 °C freezer overnight, during which brown crystals were deposited. Removal of the supernatant by a syringe and washing the crystals with hexane afforded 436 mg (0.921 mmol) in 46% yield.

Mp: 96–103 °C (dec). IR (nujol/CsI): 1070, 1020, 323, 303 cm<sup>-1</sup>. <sup>1</sup>H NMR (C<sub>6</sub>D<sub>6</sub>): δ 1.55 (s, 9H), 3.02 (s, 3H), 3.10–3.20 (m, 4H), 3.22 (s, 3H), 3.59 (s, 3H). <sup>13</sup>C{<sup>1</sup>H} NMR (C<sub>6</sub>D<sub>6</sub>): δ 25.7, 30.0, 46.0, 62.1, 67.9, 70.2, 75.9, 251.1, 263.8. Anal. Calcd for C<sub>11</sub>H<sub>22</sub>Cl<sub>3</sub>O<sub>2</sub>Ta: C, 27.90; H, 4.98. Found: C, 27.68; H, 4.82.

**TaCl<sub>5</sub>(Me<sub>3</sub>SiC≡CSiMe<sub>3</sub>)(py)<sub>2</sub> (6).** To a toluene (10 mL) solution of **1** (706 mg, 1.29 mmol) was added pyridine (208 μL, 2.58 mmol) at room temperature. The color of the reaction mixture changed to purple. After stirring the mixture at room temperature for 1 h, all volatiles were removed in vacuo and resulting purple solid was dissolved in toluene (10 mL). After centrifugation, hexane (20 mL) was slowly added to the supernatant and placed in a –20 °C freezer overnight, during which purple crystals were deposited. Removal of the supernatant by a syringe and washing the crystals with hexane afforded 476 mg (0.773 mmol) in 60% yield.



Mp: 126–131 °C (dec). IR (nujol/CsI): 1246, 1194, 1110, 1028, 983, 938, 852 cm<sup>-1</sup>. <sup>1</sup>H NMR (C<sub>6</sub>D<sub>6</sub>): δ 0.48 (s, 18H), 6.25 (t, *J* = 7.2 Hz, 6H), 6.49 (brs, 2H), 6.66 (t, *J* = 8.0 Hz, 6H), 6.80 (brs, 1H), 8.56 (d, *J* = 5.2 Hz, 2H), 9.36 (brs, 2H). <sup>13</sup>C{<sup>1</sup>H} NMR (C<sub>6</sub>D<sub>6</sub>): δ 0.8, 123.6, 124.0, 137.8, 138.5, 152.1, 152.5, 265.1. Anal. Calcd for C<sub>18</sub>H<sub>28</sub>Cl<sub>3</sub>N<sub>2</sub>Si<sub>2</sub>Ta: C, 35.14; H, 4.59; N, 4.55. Found: C, 35.17; H, 4.46; N, 4.31.

**TaCl<sub>3</sub>(Me<sub>3</sub>SiC≡CMe)(py)<sub>2</sub> (7).** To a toluene (15 mL) solution of **1** (929 mg, 1.90 mmol) was added pyridine (340 μL, 3.80 mmol) at room temperature. After stirring the mixture at room temperature for 2 h, all volatiles were removed in vacuo and the resulting purple solid was dissolved in dichloromethane (10 mL). After centrifugation, petroleum ether (20 mL) was slowly added to the supernatant and placed in a –20 °C freezer for 2 days, during which purple crystals were deposited. Removal of the supernatant by a syringe and washing the crystals with petroleum ether afforded 691 mg (1.24 mmol) in 65% yield.

Mp: 170–175 °C (dec). IR (nujol/CsI): 1644, 303 cm<sup>-1</sup>. <sup>1</sup>H NMR (C<sub>6</sub>D<sub>6</sub>): δ 0.31 (s, 9H), 3.59 (s, 3H), 6.25 (t, *J* = 6.6 Hz, 2H), 6.47 (t, *J* = 7.0 Hz, 2H), 6.67 (t, *J* = 7.7 Hz, 1H), 6.79 (t, *J* = 7.6 Hz, 1H), 8.59 (d, *J* = 5.2 Hz, 2H), 9.27 (brs, 2H). <sup>13</sup>C{<sup>1</sup>H} NMR (C<sub>6</sub>D<sub>6</sub>): δ 0.2, 28.9, 124.1, 138.5, 152.5, 250.6, 264.4. Anal. Calcd for C<sub>16</sub>H<sub>22</sub>Cl<sub>3</sub>N<sub>2</sub>SiTa: C, 34.45; H, 3.98; N, 5.02. Found: C, 33.98; H, 2.92; N, 4.96.

**TaCl<sub>3</sub>(Pr<sub>3</sub>SiC≡CMe)(dme) (8).** Toluene (5 mL) was added to TaCl<sub>5</sub> (324 mg, 0.91 mmol) in a 20 mL Schlenk tube, and then DME (2 mL) was slowly added to the resulting yellow suspension. Zn powder (71 mg, 1.09 mmol) was added to the mixture in one portion at room temperature. After stirring the mixture at room temperature for 30 min, 1-(triisopropylsilyl)-1-propyne (217 μL, 0.91 mmol) was added and the suspension was stirred at 60 °C for 1 day. The resulting insoluble inorganic salts were removed by centrifugation, and the reddish-brown supernatant was transferred to a Schlenk tube. All volatiles were removed in vacuo, and the resulting brown solid was dissolved in toluene (3 mL) and stirred for 1 day. After centrifugation, the supernatant was concentrated and hexane (5 mL) was slowly added to the supernatant. The mixture was placed in a –20 °C freezer for 4 days, during which reddish-brown crystals were deposited. Removal of the supernatant by a syringe and washing the crystals with hexane afforded 691 mg (1.24 mmol) in 16% yield.

Mp: 118–122 °C (dec). IR (nujol/CsI): 1640, 311 cm<sup>-1</sup>. <sup>1</sup>H NMR (C<sub>6</sub>D<sub>6</sub>): δ 1.37 (d, *J* = 7.6 Hz, 18H), 1.71 (sep, *J* = 7.5 Hz, 3H), 3.12 (s, 3H), 3.14–3.16 (m, 4H), 3.43 (s, 3H), 3.62 (s, 3H). <sup>13</sup>C{<sup>1</sup>H} NMR (C<sub>6</sub>D<sub>6</sub>): δ 13.4, 19.5, 30.1, 62.5, 67.8, 70.4, 75.6, 254.9, 260.8. Anal. Calcd for C<sub>16</sub>H<sub>34</sub>Cl<sub>3</sub>O<sub>2</sub>SiTa: C, 33.49; H, 5.97. Found: C, 32.97; H, 5.66.

**TaCl<sub>3</sub>(PhC≡CCOOMe)(dme) (9).** A toluene (20 mL) solution of **1** (320 mg, 0.584 mmol) and PhC≡CCOOMe (77 μL, 0.584 mmol) was heated at 50 °C for 1 day. The reaction mixture was centrifuged, and the supernatant was transferred to a Schlenk tube. All volatiles were removed under reduced pressure, and recrystallization of the residue from DME (5 mL) and petroleum ether (10 mL) at –20 °C for 2 days gave **9** (271 mg, 0.504 mmol) as pale yellow crystals in 86% yield.

Mp: 135–144 °C (dec). <sup>1</sup>H NMR (CD<sub>2</sub>Cl<sub>2</sub>): δ 3.97 (s, 3H), 4.07 (s, 3H), 4.21 (s, 3H), 4.30–4.35 (m, 4H), 7.47 (t, *J* = 7.3 Hz, 1H), 7.55 (t, *J* = 7.3 Hz, 2H), 7.82 (d, *J* = 7.1 Hz, 2H). <sup>13</sup>C{<sup>1</sup>H} NMR (CD<sub>2</sub>Cl<sub>2</sub>): δ 51.9, 63.4, 70.5, 71.6, 76.7, 128.5, 131.2, 133.0, 136.9, 228.3, 242.3. Anal. Calcd for C<sub>14</sub>H<sub>18</sub>Cl<sub>3</sub>O<sub>4</sub>Ta: C, 31.28; H, 3.37. Found: C, 31.29; H, 3.54.

**TaCl<sub>3</sub>(PhC≡CCONMe<sub>2</sub>)(py)<sub>2</sub> (10).** A toluene (30 mL) solution of **6** (348 mg, 0.565 mmol) and PhC≡CCONMe<sub>2</sub> (97.9 mg, 0.565 mmol) was heated at 80 °C for 2 days. The yellow reaction mixture was concentrated in vacuo, and the residue was extracted with dichloromethane (17 mL). The extract was concentrated, and petroleum ether (11 mL) was slowly added. Recrystallization at

–30 °C for 2 days gave **10** (158 mg, 0.254 mmol) as pale yellow crystals in 45% yield.

<sup>1</sup>H NMR (CD<sub>2</sub>Cl<sub>2</sub>): δ 3.01 (s, 3H), 3.11 (s, 3H), 7.35–8.35 (m, 12H), 8.84 (s, 1H), 9.65 (s, 2H). <sup>13</sup>C{<sup>1</sup>H} NMR (CD<sub>2</sub>Cl<sub>2</sub>): δ 30.2, 37.1, 123.7, 126.3, 127.9, 128.4, 130.9, 132.7, 134.2, 136.7, 138.7, 151.3, 186.6, 218.3, 247.3.

**Kinetic Measurement by <sup>1</sup>H NMR.** All kinetic experiments were run in a sealed NMR tube with a total solution volume of 600 μL. The reactions were heated at a constant temperature in a NMR probe in the JEOL LA400 spectrometer. A typical experimental run for the alkyne exchange reaction of **2** with diphenylacetylene is described as follows: complex **2** (19.7 mg, 40.2 μmol) and diphenylacetylene (71.7 mg, 40.2 μmol) were placed in an NMR tube using standard Schlenk techniques. Then 600 μL of C<sub>6</sub>D<sub>6</sub> was added via a syringe. The solution was quickly frozen in a dry ice–MeOH bath, and the tube was flame sealed. The frozen solution was warmed quickly in a water bath. The tube was placed in the NMR probe. At specific intervals, <sup>1</sup>H NMR spectra were recorded.

**Treatment of Kinetic Data.** An Eyring plot of ln(*k*/*T*) versus 1/*T* was made on a computer using a standard least-squares analysis. The slope and the intercept of the line were obtained directly from the computer.

**X-ray Crystallographic Analysis. Crystallographic Data Collections and Structure Determination. Data Collection.** A suitable crystal of each compound was mounted in a glass capillary under an argon atmosphere. Data for complex **9** was collected by a Rigaku AFC-7R diffractometer with graphite-monochromated Mo Kα (λ = 0.71069 Å) radiation and a 12 kW rotating anode generator. The incident beam collimator was 1.0 mm, and the crystal to detector distance was 285 mm. Cell constants and an orientation matrix for data collection, obtained from a least-squares refinement using the setting angles of 25 carefully centered reflections, corresponded to the cells with dimensions listed in Table 2, where details of the data collection are summarized. The weak reflections (*I* < 10σ(*I*)) were rescanned (maximum of 2 rescans) and the counts were accumulated to ensure good counting statistics. Stationary background counts were recorded on each side of the reflection. The ratio of peak counting time to background counting time was 2:1. Three standard reflections were chosen and monitored every 150 reflections. For complexes **1**, **2**, **7**, and **8** measurements were made on a Rigaku RAIS-IV imaging plate diffractometer with graphite-monochromated Mo Kα (λ = 0.71069 Å) radiation. The incident beam collimator was 0.8 mm, and the crystal to detector distance was 100.02 mm with the detector at the zero swing position. Indexing was performed from four oscillations, which were exposed for 4.0 min. The readout was obtained in the 0.100 mm pixel mode. A total of 45 4.00° oscillation images were collected, each being exposed for 4.0 min. Cell constants are listed in Table 2.

**Data Reduction.** An empirical absorption correction based on azimuthal scans of several reflections was applied. The data were corrected for Lorentz and polarization effects. The decays of intensities of three representative reflections were –6.57% for **9**, and thus a linear correction factor was applied to the decay of these observed data. Complexes **1**, **2**, **7**, and **8** showed no decay.

**Structure Determination and Refinement.** All calculations were performed using the TEXSAN crystallographic software package, and illustrations were drawn with ORTEP. Crystallographic calculations were performed on an SGI O2 workstation at Venture Business Laboratory, Graduate School of Okayama University. In the subsequent refinement, the function Σw(|*F*<sub>o</sub>| – |*F*<sub>c</sub>|)<sup>2</sup> was minimized, where |*F*<sub>o</sub>| and |*F*<sub>c</sub>| are the observed and calculated structure factor amplitudes, respectively. The agreement indices are defined as R1 = Σ||*F*<sub>o</sub>| – |*F*<sub>c</sub>||/Σ|*F*<sub>o</sub>| and wR2 = [Σw(|*F*<sub>o</sub>| – |*F*<sub>c</sub>|)<sup>2</sup>/Σw(|*F*<sub>o</sub>|)<sup>2</sup>]<sup>1/2</sup>. Atomic positional parameters for the non-hydrogen atoms of all complexes are given in the Supporting Information.

**Acknowledgment.** This work was supported by a Grant-in-Aid for Scientific Research on Priority Areas (No. 14078219, “Reaction Control of Dynamic Complexes”) from the Ministry of Education, Culture, Sports, Science, and Technology of Japan.

**Supporting Information Available:** CIF files for **1**, **2**, **7**, **8**, and **9** and detailed data of kinetic measurements. These materials are available free of charge via the Internet at <http://pubs.acs.org>. OM060659Z